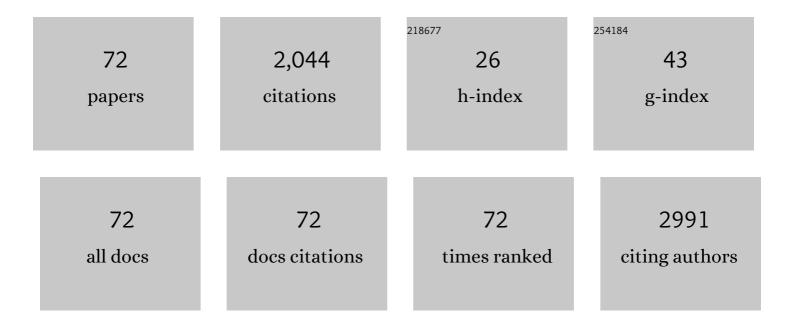
List of Publications by Year in descending order

Source: https://exaly.com/author-pdf/5814880/publications.pdf Version: 2024-02-01



#	Article	IF	CITATIONS
1	Sweat-based wearable energy harvesting-storage hybrid textile devices. Energy and Environmental Science, 2018, 11, 3431-3442.	30.8	196
2	Cooperative Assembly of Magneto-Nanovesicles with Tunable Wall Thickness and Permeability for MRI-Guided Drug Delivery. Journal of the American Chemical Society, 2018, 140, 4666-4677.	13.7	138
3	Facile synthesis of novel CuO/Cu2O nanosheets on copper foil for high sensitive nonenzymatic glucose biosensor. Sensors and Actuators B: Chemical, 2017, 248, 630-638.	7.8	113
4	A sensitive electrochemical nonenzymatic biosensor for the detection of H2O2 released from living cells based on ultrathin concave Ag nanosheets. Biosensors and Bioelectronics, 2018, 106, 29-36.	10.1	88
5	Templating synthesis of hollow CuO polyhedron and its application for nonenzymatic glucose detection. Journal of Materials Chemistry A, 2014, 2, 7306-7312.	10.3	87
6	Nanoparticle-aggregated CuO nanoellipsoids for high-performance non-enzymatic glucose detection. Journal of Materials Chemistry A, 2014, 2, 10073.	10.3	80
7	Highly symmetric polyhedral Cu2O crystals with controllable-index planes. CrystEngComm, 2011, 13, 2217.	2.6	75
8	Manipulating Cu Nanoparticle Surface Oxidation States Tunes Catalytic Selectivity toward CH ₄ or C ₂₊ Products in CO ₂ Electroreduction. Advanced Energy Materials, 2021, 11, 2101424.	19.5	71
9	Synthesis of porous carbon nano-onions derived from rice husk for high-performance supercapacitors. Applied Surface Science, 2019, 488, 593-599.	6.1	57
10	Facet-selective growth of Cu–Cu ₂ O heterogeneous architectures. CrystEngComm, 2012, 14, 40-43.	2.6	54
11	Unique polyhedral 26-facet CuS hollow architectures decorated with nanotwinned, mesostructural and single crystalline shells. CrystEngComm, 2011, 13, 6200.	2.6	39
12	Etching-limited branching growth of cuprous oxide during ethanol-assisted solution synthesis. CrystEngComm, 2011, 13, 2837.	2.6	39
13	Wearable, stable, highly sensitive hydrogel–graphene strain sensors. Beilstein Journal of Nanotechnology, 2019, 10, 475-480.	2.8	38
14	Boosting areal energy density of 3D printed all-solid-state flexible microsupercapacitors via tailoring graphene composition. Energy Storage Materials, 2020, 30, 412-419.	18.0	38
15	Yolk–Shell Cu ₂ O@CuOâ€decorated RGO for Highâ€Performance Lithiumâ€lon Battery Anode. Energy and Environmental Materials, 2022, 5, 253-260.	12.8	37
16	Surfactant-free synthesis of Cu ₂ O yolk–shell cubes decorated with Pt nanoparticles for enhanced H ₂ O ₂ detection. Chemical Communications, 2018, 54, 8458-8461.	4.1	36
17	Synthesis and Crystal-Phase Engineering of Mesoporous Palladium–Boron Alloy Nanoparticles. ACS Central Science, 2020, 6, 2347-2353.	11.3	36
18	Twins in polyhedral 26-facet Cu7S4 cages: Synthesis, characterization and their enhancing photochemical activities. Dalton Transactions, 2012, 41, 3214.	3.3	35

#	Article	IF	CITATIONS
19	Facet-dependent nonenzymatic glucose sensing properties of Cu ₂ O cubes and octahedra. New Journal of Chemistry, 2016, 40, 6573-6576.	2.8	35
20	Copper sulfide cages wholly exposed with nanotwinned building blocks. CrystEngComm, 2012, 14, 67-70.	2.6	34
21	Template-assisted synthesis of CuO hollow nanotubes constructed by ultrathin nanosheets for lithium-ion battery applications. Journal of Alloys and Compounds, 2020, 849, 156635.	5.5	34
22	Ag nanoparticles decorated PVA-co-PE nanofiber-based membrane with antifouling surface for highly efficient inactivation and interception of bacteria. Applied Surface Science, 2020, 506, 144664.	6.1	32
23	Selective-etching growth of urchin-like Cu2O architectures. CrystEngComm, 2011, 13, 6616.	2.6	31
24	Ultrafine RhNi Nanocatalysts Confined in Hollow Mesoporous Carbons for a Highly Efficient Hydrogen Production from Ammonia Borane. Inorganic Chemistry, 2021, 60, 6820-6828.	4.0	31
25	Facile hydroxyl-assisted synthesis of morphological Cu ₂ O architectures and their shape-dependent photocatalytic performances. New Journal of Chemistry, 2014, 38, 4656-4660.	2.8	30
26	Seed-mediated synthesis of polyhedral 50-facet Cu2O architectures. CrystEngComm, 2011, 13, 5993.	2.6	29
27	Template-synthesis of hierarchical CuO nanoflowers constructed by ultrathin nanosheets and their application for non-enzymatic glucose detection. Materials Letters, 2018, 219, 134-137.	2.6	27
28	CuO ultrathin nanosheets decorated reduced graphene oxide as a high performance anode for lithium-ion batteries. Journal of Alloys and Compounds, 2019, 805, 355-362.	5.5	27
29	Inter-embedded Au-Cu2O heterostructure for the enhanced hydrogen production from water splitting under the visible light. Chemical Engineering Journal, 2021, 405, 126709.	12.7	27
30	Polymeric Ligand-Mediated Regioselective Bonding of Plasmonic Nanoplates and Nanospheres. Journal of the American Chemical Society, 2020, 142, 17282-17286.	13.7	25
31	Localized surface plasmon enhanced electrocatalytic methanol oxidation of AgPt bimetallic nanoparticles with an ultra-thin shell. Chemical Communications, 2019, 55, 3943-3946.	4.1	24
32	Nanoparticle-aggregated paddy-like copper dendritic nanostructures. CrystEngComm, 2011, 13, 1916-1921.	2.6	23
33	Nanoparticle-aggregated hollow copper microcages and their surface-enhanced Raman scattering activity. CrystEngComm, 2013, 15, 6136.	2.6	23
34	Polyhedron-aggregated multi-facet Cu2O homogeneous structures. CrystEngComm, 2011, 13, 6040.	2.6	22
35	Zinc ion mediated synthesis of cuprous oxide crystals for non-enzymatic glucose detection. Journal of Materials Chemistry B, 2017, 5, 8686-8694.	5.8	21
36	Intrinsic insight on localized surface plasmon resonance enhanced methanol electro-oxidation over a Au@AgPt hollow urchin-like nanostructure. Journal of Materials Chemistry A, 2020, 8, 6638-6646.	10.3	19

#	Article	IF	CITATIONS
37	One-pot synthesis of etched Cu ₂ O cubes with exposed {110} facets with enhanced visible-light-driven photocatalytic activity. Physical Chemistry Chemical Physics, 2015, 17, 29479-29482.	2.8	18
38	Immobilized Seed-Mediated Growth of Two-Dimensional Array of Metallic Nanocrystals with Asymmetric Shapes. ACS Nano, 2018, 12, 1107-1119.	14.6	18
39	Cu–Cu ₂ 0 Heterogeneous Architecture for the Enhanced CO Catalytic Oxidation. Advanced Materials Interfaces, 2020, 7, 1901643.	3.7	17
40	Nanoparticle-aggregated octahedral copper hierarchical nanostructures. CrystEngComm, 2011, 13, 63-66.	2.6	16
41	Nanocube-aggregated cauliflower-like copper hierarchical architectures: synthesis, growth mechanism and electrocatalytic activity. CrystEngComm, 2012, 14, 5737.	2.6	16
42	A Readily Accessible Functional Nanofibrous Membrane for Highâ€Capacity Immobilization of Ag Nanoparticles and Ultrafast Catalysis Application. Advanced Materials Interfaces, 2019, 6, 1801617.	3.7	15
43	Templated-synthesis of hierarchical Ag-AgBr hollow cubes with enhanced visible-light-responsive photocatalytic activity. Applied Surface Science, 2018, 443, 492-496.	6.1	14
44	Controllable inâ€situ Synthesis of Cu–Cu ₂ O Heterostructures with Enhanced Visibleâ€light Photocatalytic Activity. ChemistrySelect, 2018, 3, 10641-10645.	1.5	13
45	Modified thermal resistance networks model for transverse thermal conductivity of unidirectional fiber composite. Composites Communications, 2017, 6, 52-58.	6.3	12
46	Reaction mechanism, norbornene and ligand effects, and origins of meta-selectivity of Pd/norbornene-catalyzed C–H activation. Chemical Science, 2020, 11, 113-125.	7.4	11
47	2D hydrogenated boride as a reductant and stabilizer for <i>in situ</i> synthesis of ultrafine and surfactant-free carbon supported noble metal electrocatalysts with enhanced activity and stability. Journal of Materials Chemistry A, 2020, 8, 18856-18862.	10.3	11
48	An Mn ²⁺ -mediated construction of rhombicuboctahedral Cu ₂ O nanocrystals enclosed by jagged surfaces for enhanced enzyme-free glucose sensing. CrystEngComm, 2020, 22, 2042-2048.	2.6	11
49	Atomically ordered Rh ₂ P catalysts anchored within hollow mesoporous carbon for efficient hydrogen production. Chemical Communications, 2021, 57, 12345-12348.	4.1	11
50	One-pot synthesis of ultrafine Ag-hydrogel composites with enhanced catalytic reduction of 4-nitrophenol. Materials Letters, 2019, 236, 530-533.	2.6	10
51	Cu2O-based binary and ternary photocatalysts for the degradation of organic dyes under visible light. Ceramics International, 2022, 48, 1757-1764.	4.8	10
52	Designated-Tailoring on {100} Facets of Cu ₂ O Nanostructures: From Octahedral to Its Different Truncated Forms. Journal of Nanomaterials, 2010, 2010, 1-11.	2.7	8
53	Magnetic field driven assembly of 1D-aligned silver superstructures. CrystEngComm, 2011, 13, 4827.	2.6	8
54	Low-Cost Synthetic Honeycomb-like Carbon Derived from Cotton as a Sulfur Host for the Enhanced Electrochemical Performances of Lithium–Sulfur Batteries. Energy & Fuels, 2020, 34, 13096-13103.	5.1	8

#	Article	IF	CITATIONS
55	CoFe Nanoparticle-Decorated Reduced Graphene Oxide for the Highly Efficient Reduction of 4-Nitrophenol. Langmuir, 2021, 37, 10987-10993.	3.5	8
56	Copper-templated synthesis of gold microcages for sensitive surface-enhanced Raman scattering activity. RSC Advances, 2014, 4, 27074-27077.	3.6	7
57	Continuous UV irradiation synthesis of ultra-small Au nanoparticles decorated Cu2O with enhanced photocatalytic activity. Composites Communications, 2018, 9, 27-32.	6.3	6
58	Ultrathin CuxO nanoflakes anchored Cu2O nanoarray for high-performance non-enzymatic glucose sensor. Journal of Solid State Electrochemistry, 2020, 24, 583-590.	2.5	6
59	RGO@Cu2O@Cu Ternary Nanocomposite for High-Performance Non-Enzymatic Glucose Detection. Journal of the Electrochemical Society, 2021, 168, 087503.	2.9	6
60	Endohedral group-14-element clusters TM@E ₉ (TM = Co, Ni, Cu; E = Ge, Sn, Pb) and their low-dimensional nanostructures: a first-principles study. Physical Chemistry Chemical Physics, 2021, 23, 20654-20665.	2.8	6
61	Stable Noble Gas Compounds Based on Superelectrophilic Anions [B ₁₂ (BO) ₁₁] ^{â^`} and [B ₁₂ (OBO) ₁₁] ^{â^`} . ChemPhysChem, 2021, 22, 2240-2246.	2.1	5
62	Enhancement of energy storage properties of Bi0.5Na0.5TiO3-based relaxor ferroelectric under moderate electric field. Applied Physics Letters, 2022, 120, .	3.3	5
63	Nanosized nickel decorated sisal fibers with tailored aggregation structures for catalysis reduction of toxic aromatic compounds. Industrial Crops and Products, 2018, 119, 226-236.	5.2	4
64	Manipulating Cu Nanoparticle Surface Oxidation States Tunes Catalytic Selectivity toward CH ₄ or C ₂₊ Products in CO ₂ Electroreduction (Adv. Energy) Tj ETQq0 0 C) r g:₿1 5/Ove	erløck 10 Tf 5
65	Geometries, electronic structures, and bonding properties of endohedral Groupâ€14 Zintl clusters <scp>TM</scp> @ <scp>E₁₀</scp> (<scp>TM</scp> = Fe, Co, Ni; E = Ge, Sn, Pb). Journal of Computational Chemistry, 2022, 43, 828-838.	3.3	3
66	Stabilities, Electronic Structures, and Bonding Properties of Iron Complexes (E 1 E 2)Fe(CO) 2 (CNAr) Tj ETQq0 C	0.rgBT /0	verlock 10 T
67	Stabilities, Electronic Structures, and Bonding Properties of 20-Electron Transition Metal Complexes (Cp) ₂ TMO and their One-Dimensional Sandwich Molecular Wires (Cp =) Tj ETQq1 1 0.784314 rgBT	/Overlock 2.5	10 Tf 50 267 2
68	125, 721 730. Caterpillar-like Ag–ZnO–C hollow nanocomposites for efficient solar photocatalytic degradation and disinfection. Environmental Science: Nano, 2022, 9, 975-987.	4.3	2
69	Rapid Oxidation Synthesis of Hollow Cupric Oxide-Decorated rGO with High Performance and Kinetically Enhanced Lithium Storage. Energy & Fuels, 0, , .	5.1	1
70	Novel Design of 3-D Microstructure Contact Material Generating Autoexcitation Magnetic Field. IEEE Transactions on Plasma Science, 2021, 49, 1969-1974.	1.3	0
71	Theoretical Insight into 20â€Electron Transition Metal Complexes (C ₅ H ₅) ₂ TM(E ₁ E ₂) ₂ (TM =â€ Bonding Nature, Physica Status Solidi (B): Basic Research, 2021, 258, 2100417.	‰Cr,) Tj E 1.5	TQq1 1 0.78
72	Designing stable <i>closo</i> B ₁₂ dianions <i>in silico</i> for Li- and Mg-ion battery applications. Inorganic Chemistry Frontiers, 2021, 8, 5201-5208.	6.0	0